J Mater Sci: Mater Med (2006) 17:815–823
DOI 10.1007/s10856-006-9840-3

Characterization and osteoblast-like cell compatibility of porous scaffolds: bovine hydroxyapatite and novel hydroxyapatite artificial bone

Yuan Gao · Wen-Ling Cao · Xiao-Yan Wang · Yan-Dao Gong · Jie-Mo Tian · Nan-Ming Zhao · Xiu-Fang Zhang

Received: 5 November 2004 / Accepted: 21 October 2005

Abstract Three different porous scaffolds were tested. The first two were prepared by sintering bovine bone. The third scaffold was prepared using three-dimensional gel-lamination, a new rapid prototyping method, and was named as hydroxyapatite artificial bone.

X-ray diffraction and Fourier transform infrared spectroscopy analysis confirmed that the samples were mainly highly crystalline hydroxyapatite ceramics. Scanning electron microscopy and mercury intrusion porosimetry measurement showed that the pores were interconnected and pore sizes ranged from several microns to hundreds of microns.

Mouse osteoblast-like cells grown on the three scaffolds retained their characteristic morphology. Cell proliferation and differentiation, analyzed by methylthiazol tetrazolium (MTT) and alkaline phosphatase activity assays, were significantly higher on the hydroxyapatite artificial bone than on the other two scaffolds tested. All the scaffolds provided good attachment, proliferation and differentiation of bone cells.

These results indicate that the scaffolds have a favorable interaction with cells, they support cell growth and functions, and therefore these scaffolds may have great potential as bone substitutes. The three-dimensional gel-lamination method is proven to be an attractive process to design and fabricate bone scaffolds with favorable properties, and therefore, has promising potential for bone repair applications.

Y. Gao · W.-L. Cao · Y.-D. Gong · N.-M. Zhao · X.-F. Zhang (✉)
Department of Biological Sciences and Biotechnology, State Key Laboratory of Biomembrane and Membrane Biotechnology, Tsinghua University, Beijing 100084, China
e-mail: zxf-dbs@mail.tsinghua.edu.cn

X.-Y. Wang · J.-M. Tian
Institute of Nuclear Energy Technology, Tsinghua University, Beijing 100084, China

1. Introduction

Tumors, trauma, disease and birth defects create a demand for skeletal reconstruction. Although autograft and allograft are the standard treatments, they are sometimes accompanied by problems of donor site scarcity, rejection by the immune system, resorption and pathogen transfer. Therefore, many investigations have been conducted to find materials for bone substitutes. Among them, hydroxyapatite (HA) is perhaps one of the most promising materials.

HA is the major mineral component of bone and teeth, with a chemical formula of $Ca_{10}(PO_4)_6(OH)_2$. It can promote faster bone regeneration and direct bonding to regenerated bone without intermediate connective tissue [1, 2]. Due to their excellent biocompatibility and bioactivity, HA ceramics have been widely used in bone grafting and dental devices as bone substitutes and since the discovery of their osteoinductivity, have attracted much interest in the field of biomaterial research in the past decade [3–6]. HA ceramics have the ability to induce mesenchymal cells to differentiate toward osteoblasts, which makes HA a good scaffold material for bone tissue engineering [7–9].

Biological studies and clinical practice have established that in addition to the requirements for compositional properties of a material, a three-dimensional (3-D) interconnected porous structure is necessary to provide space for tissue development and to offer temporary mechanical support. Porous biomimetic matrices may provide a suitable microenvironment that promotes osteoblast attachment, proliferation and differentiation. Therefore, a number of techniques have been developed to fabricate porous HA scaffolds, typically

including the incorporation of volatile organic particles in the HA powder, gel casting of foams, and replication of a polymer sponge [10, 11].

Hydroxyapatite ceramics manufactured from coral or bovine bone retain their chemical composition of bone mineral and have the advantage of inheriting some properties of the raw materials such as the pore structure [12–14]. Moreover, they are easily available and have a lower cost than autogenetic or allogenetic bone grafts.

In this study, a 3-D gel-lamination system, which is a new rapid prototyping technology, was used for the preparation of porous HA scaffolds. Based on the incorporation of rapid prototyping technology and gelcasting, the 3-D gel-lamination process provides an innovative concept for customized construction of artificial bone [15].

The structural and chemical properties of three HA porous materials were studied; two of them were obtained by sintering of bovine bone and the third one by the 3-D gel-lamination method. Afterwards, the three materials were inoculated with osteoblast-like cells in order to evaluate their biocompatibility and the cells behavior.

2. Materials and methods

2.1. Materials

Alpha-minimum essential medium (α-MEM), fetal bovine serum (FBS) and trypsin were purchased from GIBCO (Grand Island, NY, USA). Ascorbic acid and β-glycerophosphate were purchased from Sigma (St. Louis, MO, USA). D-9300 (Beijing Eastern Rohm & Haas Co., Ltd, China) was used as dispersant. Sodium alginate (Beijing Xudong Chemical Plant, China) was adopted as the gelling polymer, and calcium chloride was chosen as the initiator. All other materials were of reagent grade.

2.2. Scaffold preparation

Three different HA-based porous materials were tested. Two of them, scaffolds A and B, were manufactured by sintering of bovine bone. The third one, scaffold C, was fabricated using a new rapid prototyping method, 3-D gel-lamination. All of the specimens were $1.0 \times 1.0 \times 0.2$ cm in size.

2.2.1. A and B scaffolds

Fresh bovine cancellous bone was cut into pieces of $1.0 \times 1.0 \times 0.2$ cm, and stored at -20°C until treatment. To eliminate the organic components in the bone scaffold, it was immersed in 30% hydrogen peroxide for 24 h. Then the samples were degreased by immersion in ether for 24 h. After dehydration through a series of ethanol treatments with increasing concentrations, the scaffolds were dried at 100–120°C. Finally, scaffolds A and B were obtained by sintering of bone scaffolds at 1120°C and 1350°C for 3–5 h, respectively.

2.2.2. C scaffolds

Scaffold C was fabricated by a three-dimensional gel-lamination technique which has been described previously [15]. HA powder served as the ceramic phase. HA powder was synthesized via chemical precipitation from the aqueous solutions of triammonium phosphate trihydrate and calcium nitrate tetrahydrate. The synthetic HA powder was calcined at 900°C for 24 hours, and the average size of the HA particles was about 1.52 μm.

The HA powder was mixed together with deionized water and dispersant to form a ceramic slurry with 45 vol% solids loading by means of ball milling within a polyethylene jar. Prior to the 3-D gel-lamination process, 4 wt% sodium alginate solution was blended with the slurry. The prepared slurry was degassed and then infused into the slurry pond of the 3-D gel-lamination machine. With the 3-D gel-lamination machine, a green specimen was obtained. Then the specimens were dried slowly at room temperature with high humidity. After drying, they were heated at 300–500°C at a reasonably slow heating rate to burn out the organic material, followed by sintering at 1150°C for 3 h.

2.3. Fourier transform infrared spectroscopy (FT-IR)

The samples were pressed into pellets with KBr. Then the IR spectra was measured using a FT-IR Spectrometer (model Spectrum GX; Perkin-Elmer) in the wavelength range of 4000–400 cm^{-1}.

2.4. X-ray diffraction (XRD)

The phase composition of samples was determined by an X-ray Diffractometer (model D8 Advance; Bruker) with Ni-filtered Cu radiation generated at 30 kV and 30 mA as the X-ray source. The diffraction patterns were determined over a range of 20 to 60°2θ angle at a rate of 1° per min and a step size of 0.1°. Spectra were compared with the literature profiles of the Joint Committee on Powder Diffraction Standards (JCPDS) to identify the compounds.

2.5. Scanning electron microscopy (SEM)

The HA scaffolds were examined using a scanning electron microscope (KYKY-2800, Chinese Academy of Science, Beijing, China) with an acceleration voltage of 20–25 kV. Before the observation, the specimens were mounted on aluminium stumps and coated with gold in a sputtering device for 180 s under vacuum.

The osteoblast-like cells cultured on HA scaffolds were washed three times after 7 days of culture with phosphate buffered saline (PBS), followed by fixing with 3% glutaraldehyde in PBS for 12 h at 4°C. The specimens were then washed three times with PBS, followed by post-fixation with 1% osmium tetroxide in distilled water for 1 h at 4°C. After fixation, the specimens were dehydrated in increasing concentrations of ethanol (from 50%, 70%, 80%, 90%, 95% to 100%), followed by lyophilization and then observation by SEM.

2.6. Porosity and density measurements

Samples were introduced into a 6 cm^3 pycnometer, which was precisely weighed. The porosity of the scaffolds was estimated using a mercury porosimeter (Porosimeter 2000°C AutoPore IV 9510°C Micromeritics Corporation Instrument, US), providing the total porous volume (V_p), the special pore area (S_p), and the pore size distribution. The measurements were performed between 0.1 psia to 60000 psia (under low pressure and high pressure). A 10s equilibration time was to set for each intermediate data point. At each equilibration point, mercury intrusion data was recorded and plotted against pressure. For data interpretation, a contact angle of 130° and a surface tension of 0.485 Nm^{-1} were used. The porosity ε was calculated from the total intrusion volume per unit mass (Vi) and sample density (ρ_0) according to the following relationship:

$$\varepsilon = \mathrm{Vi} / (\mathrm{Vi} + \mathrm{l}/\rho_0).$$

The true density of the samples was determined on an AccuPyc 1330 (Micromeritics; Norcross, GA, USA) helium gas pycnometer. The volume of the samples was determined by measuring the pressure change of helium in a calibrated volume. If the sample weight has been specified, true density can be derived automatically. The reported density was the average of five measurements taken at 22 ± 1°C.

2.7. Osteoblast affinity

MC3T3-E1 cells were obtained from RIKEN Cell Bank (Tokyo, Japan). These immature osteoblast-like cells express osteoblast-specific proteins and produce mineralized nodules during *in vitro* maturation and have been used as a model for osteoblast growth and differentiation [16, 17].

Prior to cell seeding, the scaffolds were ultrasonically cleaned and then prewetted with 70% ethanol overnight to sterilize them and enhance their water uptake [18]. Ethanol was removed by washing the scaffolds three times with phosphate-buffered saline (PBS) for 1 h. The scaffolds were then exposed to UV light (15 w UV sterilamp, Philips) for 2 h, and finally soaked in medium containing 10% fetal bovine serum (FBS) for 12 h.

2.7.1. Cell culture

MC3 T3-E1 cells were cultured in α-MEM supplemented with 10% FBS, 100 U/ml penicillin, and 100 μg/ml streptomycin. Cells were maintained at 37°C in a 5% CO_2 incubator and the medium was changed every 3 days. For experiments, aliquots of 50 μl cell suspensions were seeded onto the top of prewetted scaffolds placed in the wells of 24-well plates, resulting in a density of 1.0×10^5 cells per scaffold. The scaffolds were left undisturbed in an incubator for 3 h to allow full attachment of cells to scaffolds, after which time an additional 1 ml of complete medium was added to each well. Complete medium was changed every 3 days. At least three specimens were used in each analysis. Unseeded scaffolds were also treated in the same manner and used as controls.

To induce cell differentiation, MC3T3-E1 cells cultured on HA scaffolds were fed with complete medium containing 10 mM β-glycerophosphate and 50 μg/ml ascorbic acid.

2.7.2. Cell proliferation

After cell growing for 1, 3, 7, or 10 days, the proliferation of MC3T3-E1 cells was determined by methylthiazol tetrazolium (MTT) assay, which measured mitochondrial dehydrogenase activity of viable cells spectrophotometrically [19].

Briefly, 1 ml serum free medium and 100 μl MTT solution (5 mg/ml in PBS) were added to each well. After 4 h incubation at 37°C, 250 μl 10% SDS (Sigma, USA) in 0.01 M HCl was added. The scaffolds were then broken up with a pipette tip to improve the dissolution of formazan crystals. After 12 h, fine ceramic fragments were removed by centrifugation at 18000 g for 10 min. The optical density (OD) at 570 nm was determined against SDS solution blank. MTT assay was first performed on a directly counted MC3 T3-E1 cell serial (0.2×10^6, 0.4×10^6, 0.8×10^6, 1.6×10^6, 3.2×10^6, 8×10^6), and the absorbency values were plotted against the counted cell numbers to establish a standard calibration curve. Viable cell numbers on scaffolds were then determined from the standard curve based on their MTT absorbency.

2.7.3. Alkaline phosphatase (ALP) activity

The differentiation of cells to osteoblasts was evaluated with the expression of ALP. The ALP activity was evaluated on the transformation of p-nitrophenyl phosphate into p-nitrophenol at pH 10.2.

MC3T3-E1 cells were cultured with HA scaffolds for 7, 14, 21, or 28 days. At the end of each incubation period, the cell cultures were washed three times with PBS. To process material for the analysis of ALP activity, 250 μl of cell lysis solution (0.5% v/v Triton X-100, 50 mM Tris

(pH 7.6), 1 mM $MgCl_2$) was added to each well containing a cell-scaffold sample. The scaffolds were broken up with a pipette tip to improve cell lysis, and they were then frozen and thawed three times. After the final thaw, the cell lysates were centrifuged for 10 min at 18000 g. The supernatants were then incubated with the Alkaline Phosphatase reagent (Sigma, Cat # 245) at 37°C and the ALP activity was spectrophotometrically measured at 405 nm. Data was normalized for total cell protein measured with the BCA Protein Assay Reagent Kit (Pierce Chemical Co., Rockford, IL, USA). Thus, the ALP activity was expressed as units per gram of protein.

2.8. Statistical analysis

Results of density, MTT and ALP assays were expressed as means ± standard deviation (SD). After the assessment of significant differences by one-way analysis of variance (ANOVA), differences among groups were established with t-test analysis by a two population comparison. *P*-values < 0.05 were considered statistically significant.

3. Results

3.1. FT-IR spectrum analysis

The functional groups present in the samples were determined by FT-IR spectroscopy. Fig. 1 shows FT-IR spectra of scaffolds A, B and C. IR bands at 3571 and 637 cm^{-1} were assigned to hydroxyl group stretching and librational modes, respectively, and the bands at 1090 and 1040, 960, and 600 and 570 cm^{-1} were assigned to v_3, v_1 and v_4 phosphate group modes, respectively. The analyses of these samples revealed only reflections corresponding to the HA phase [20, 21]. The presence of vibrations due to other impure phases was not detected. However, the peak at 637 cm^{-1} disappeared for scaffold B, which was sintered at 1350°C.

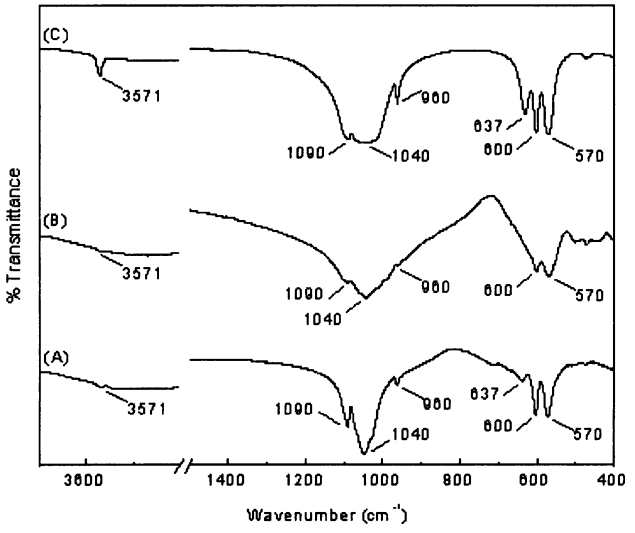

Fig. 1 FT-IR spectra of HA samples. Scaffolds A and B were prepared by sintering of bovine bone at 1120°C and 1350°C, respectively; scaffold C by the three-dimensional gel-lamination method.

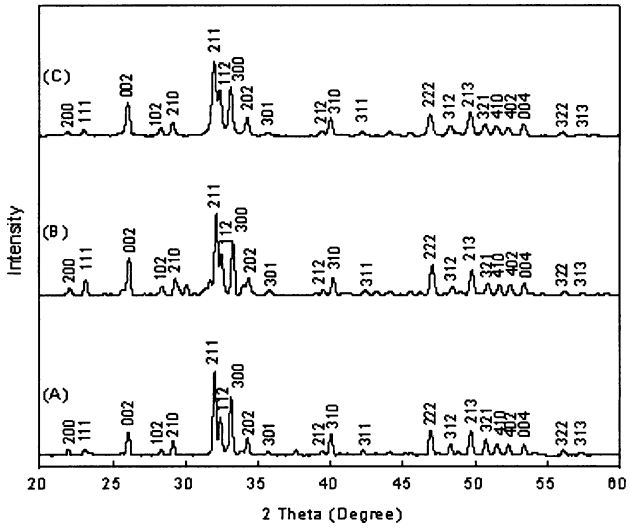

Fig. 2 XRD patterns of HA samples.

3.2. XRD pattern

The crystalline phases present in the samples were identified by XRD. As shown in Fig. 2, XRD analysis of the three samples revealed mainly a phase of HA, with the peaks matching JCPDS standards (9-432). Moreover, the peaks were sharp and distinct, which indicated that those samples were highly crystalline materials.

3.3. Surface morphology

SEM observations revealed that all the scaffolds had a highly porous, well-interconnected pore structure (Fig. 3). Individual grains were largest in scaffold B, which was sintered at 1350°C. This can be explained as a consequence of the coalescence and grain growth occurring on sintering that caused the smallest pores to close first [22]. The SEM micrograph exhibited that scaffold C had the densest microstructure.

3.4. Porosity and density

The density of HA scaffolds varied both with sintering temperature and methods of preparation (Fig. 4). For scaffolds A and B, the true densities measured were 3.100 ± 0.005 and 3.040 ± 0.010 g/cm^3, respectively, and the density decreased slightly as the sintering temperature was increased. The maximum density of 5.120 ± 0.083 g/cm^3 in this study

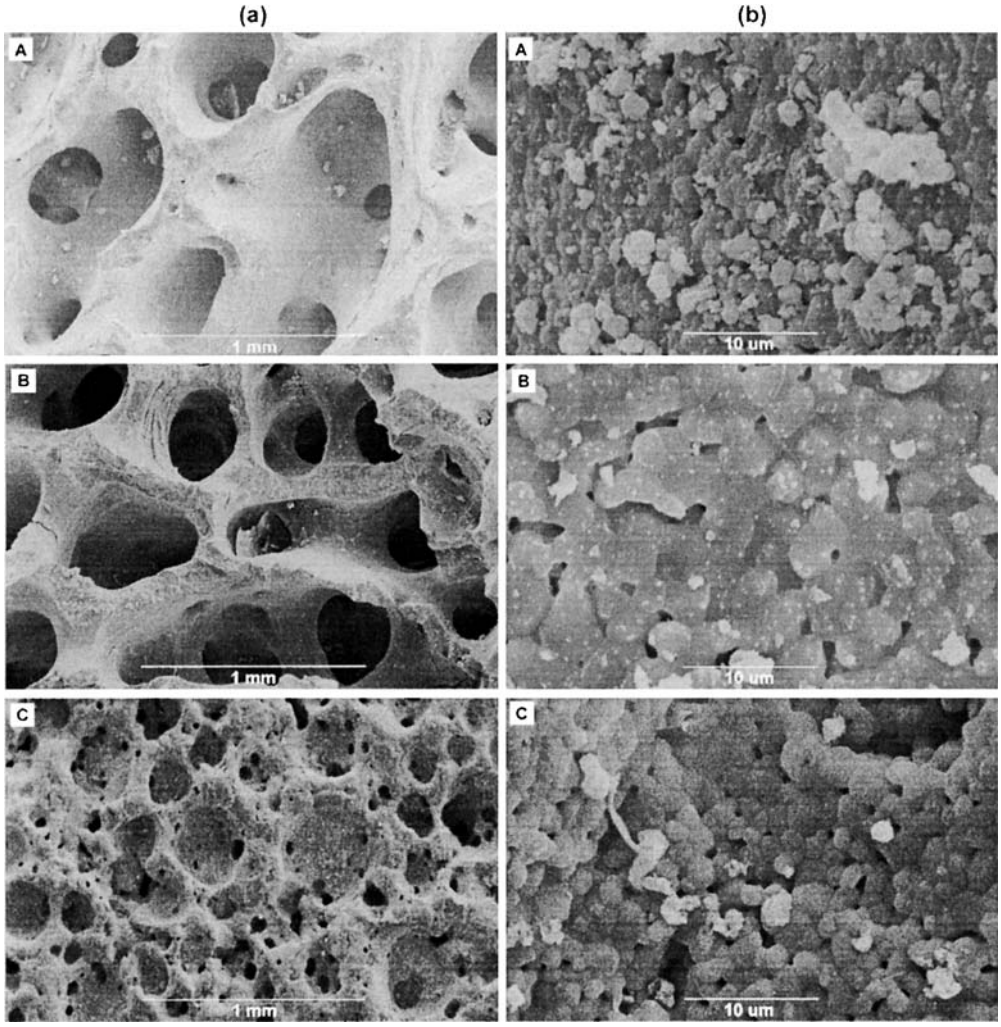

Fig. 3 SEM micrographs of HA samples. Magnifications were × 50 (series a) and × 3000 (series b)

was achieved for scaffold C. Large pores were observed by SEM examination for scaffolds A and B, which explained why they showed a lower true density.

The mercury intrusion method was used to confirm that scaffolds A, B and C were highly porous, with porosities of approx. 72%, 62% and 85%, respectively (Fig. 4). For scaffolds A and B, there was a gradual reduction in porosity as the sintering temperature was increased.

The porosimetry data (Fig. 5) describes the distribution of pore sizes. For scaffolds A and B, the pore sizes mainly distributed around 309 and 311 μm, respectively. Both scaffolds A and B had a pore size ranging from several microns to several hundreds of microns, similar to the natural structure of bone and which seems to be preserved during manufacturing [23]. The preparation of scaffold C followed a different procedure and consequently the pore distribution also followed a different pattern. Scaffold C showed a broad range of pore sizes and appeared to have a bimodal distribution, the major contribution being centred at 60 μm, and a less important one at around 458 μm. These micropores, generally at sizes around 60 μm, are critically important in facilitating the circulation of body fluid which further supplies the necessary nutrients and mineral ions for biological functions [24].

3.5. Cell morphology

After 7 days of culturing, the osteoblast-like cells reach confluency on the surface of all the HA scaffolds. Most of the cells were flattened, polygonally shape and spread, showing numerous, highly extended filipodia and rough dorsal surfaces characteristic of active cells, as shown in Fig. 6.

At higher magnification, an osteoblast cell process can be seen intimately associated with an extensive network of fibrillar and globular substances, which were suspected to be the deposition of collagen and other extracellular matrix components synthesized and organized by the osteoblast-like cells.

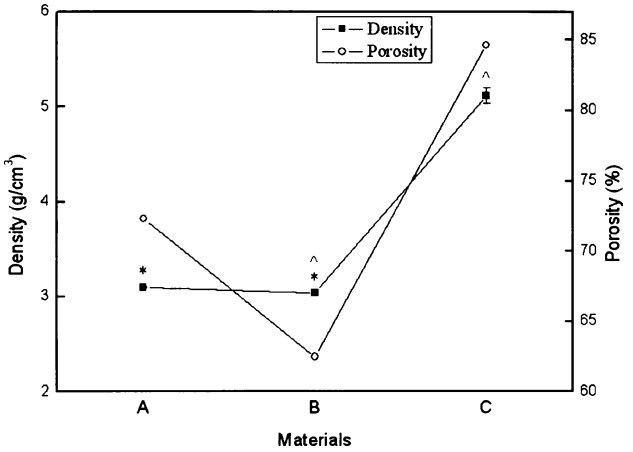

Fig. 4 Density and porosity of HA samples. The values of density were expressed as means ± standard deviation (SD) of five measurements; $^{*}p < 0.05$ compared with scaffold C, $^{\wedge}p < 0.05$ compared with scaffold A.

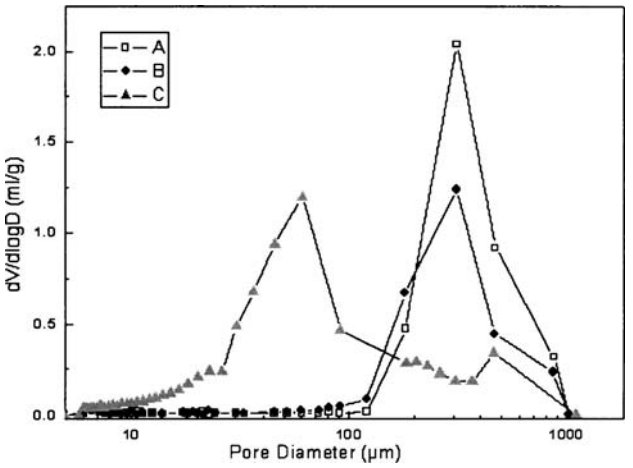

Fig. 5 Pore size distribution for HA samples. Y-coordinate (dV/dlogD) is the differential pore volume versus the logarithmic value of pore diameter.

No obvious differences in morphology were noted among the cells grown on any of the HA scaffolds.

3.6. MTT assay

Osteoblast-like cell proliferation was seen to increase on all HA scaffolds from days 1 to 10 evaluated by an MTT test. As indicated in Fig. 7, osteoblast proliferation was similar on scaffolds A and B, and the rate of proliferation on scaffold C was greater among all the scaffolds ($p < 0.05$).

Although the number of cells on the surface of scaffold C was significantly smaller on day 1 ($p < 0.05$), there was no significant difference in any of the scaffolds on day 3. In contrast, a statistically significant increase in proliferation was measured for osteoblast-like cells on scaffold C than on scaffolds A and B after 7 and 10 days of culture, respectively ($p < 0.05$). These results indicated that osteoblast-like cells responded well to scaffold C.

3.7. ALP activity

ALP is a representative enzyme of osteoblastic differentiation, and ALP activity was determined as an indicator of osteoblastic differentiation of MC3T3-E1 cells cultured on HA scaffolds.

As shown in Fig. 7, ALP activity of cells grown on all specimens increased continuously over the observation period. On day 7 and day 14, the ALP activity on HA scaffolds was low, and then increased on day 21 and day 28. The ALP activity of osteoblast-like cells grown on scaffolds A and B for various culture times was significantly lower than that of scaffold C ($p < 0.05$). In particular, scaffold A exhibited an ALP expression level similar to scaffold B.

4. Discussion

We fabricated scaffold C using a new rapid prototyping technique, three-dimensional gel-lamination. Scaffolds A and B were manufactured by sintering of bovine bone at 1120°C and 1350°C, respectively.

Although scaffolds A and B were derived from biological origins, due to the high temperature process, they are free from antigenic response.

The composition of these scaffolds was determined by FT-IR and XRD. Both methods showed these scaffolds had HA characteristics.

Highly crystalline surfaces have been reported to be more resistant to dissolution by body fluids than amorphous surfaces [25]. Some authors reported that HA materials with higher crystallinity yielded higher rates of cell proliferation [26].

Furthermore, changes in degree of crystallinity and phase purity may also lead to variations in the level of specimen solubility, which would affect scaffold degradation [27–29]. Thus, preserving the phase composition and crystalline structure of HA during sintering becomes critical for its biological applications. The high thermal stability of HA materials shown in this study makes a fully densified structure possible at high sintering temperatures.

Even though differences in pore size for all three samples within a large range (from several microns to several hundreds of microns) did not significantly affect bone cells proliferation or function *in vitro*, Tachibana *et al.* have found that a homogeneous porous scaffold with a pore size of 100 μm is suitable for high-density cultivation of cells (over 7 million cells on 1-cm diameter scaffold) [30]. However, other

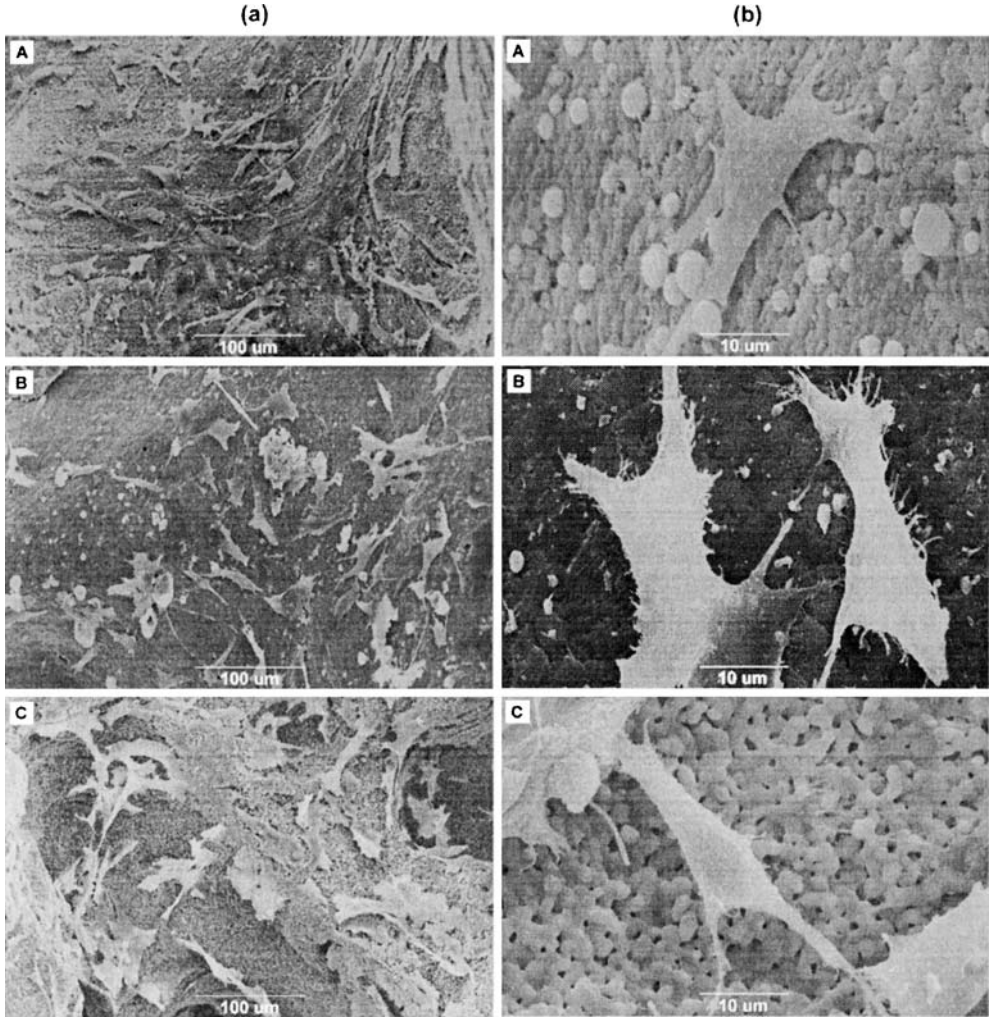

Fig. 6 SEM micrographs of MC3T3-E1 cells cultured on HA scaffolds for 7 days. Magnifications were × 250 (series a) and × 2000 (series b)

studies have demonstrated that for sufficiently rapid growth of cells, a pore size of 300–500 μm is required [31, 32].

An interconnected open pore structure is also essential for a material to serve as a temporary scaffold for bone tissue because it favors body fluid circulation and bone protein adsorption, which enhance osteoconduction; it also promotes bone ingrowth and reconstruction [33–35].

The apparent density of a porous scaffold can influence its mechanical strength and permeability [36]. The mechanical properties of a porous material depend on the density of the pore wall material as suggested by Gibson [37]. The higher density of scaffold C possibly leads to greater mechanical strength than scaffolds A and B.

Generally, established cell lines have been used as *in vitro* models for testing biocompatibility because they are readily available in large numbers and their genetic uniformity of phenotype and function produces more reproducible assays and reduces variability within and between laboratories.

To assess the cellular response, osteoblast-like cells (MC3T3-E1) were cultured on the HA scaffolds. The cells adhered well to the material as confirmed by SEM observation. The MTT and ALP results showed normal osteoblastic trends with an initial high level of proliferation, followed by a subsequent increase in ALP activity [38, 39].

The significant difference of osteoblast adhesion and spreading on the analyzed materials depends on the differences in chemical composition and topography of substrates [40–43]. Cell attachment was also dependent on surface roughness. The number of adherent cells per unit surface of HA increased with increase of the surface roughness [43].

The present study indicates that scaffolds A and B showed better cell attachment than C. Despite the initial delay in cell growth on scaffold C, the MC3T3-E1 cells nevertheless appeared to recover and proliferated at the greatest rate among all the scaffolds. All of the samples were composed of apatite, and besides, the crystallinities of the samples were similar. Therefore, the differences of cell attachment and

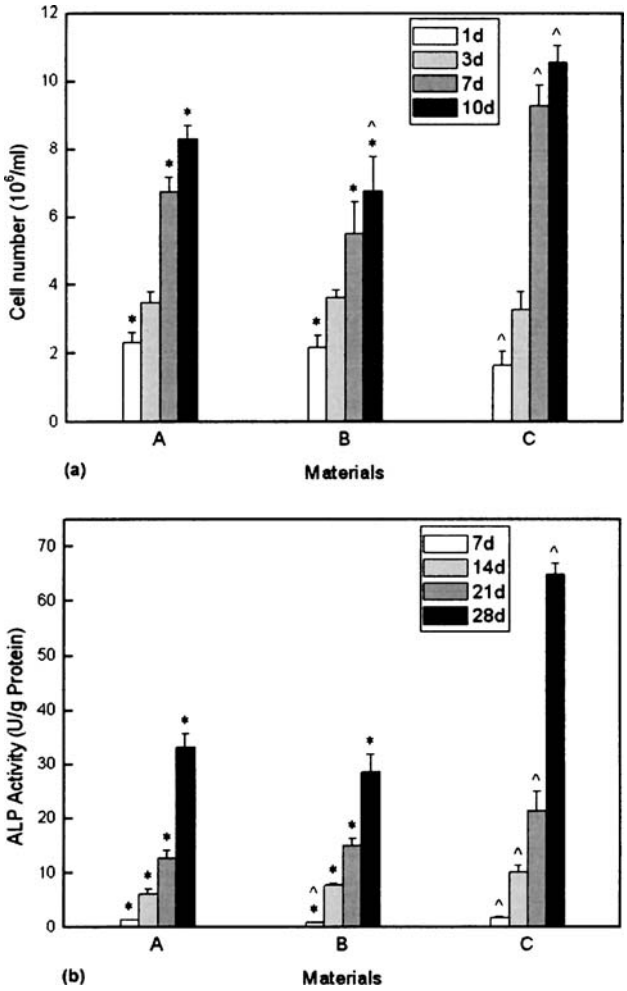

Fig. 7 Proliferation (a) and ALP activity (b) of MC3T3-E1 cells on HA scaffolds after various culture times. Results of MTT and ALP assays were expressed as means ± standard deviation (SD) of three cultures; $^*p < 0.05$ compared with scaffold C, $^\wedge p < 0.05$ compared with scaffold A at the corresponding time point.

cellular multiplication on three scaffolds were not likely to be caused by the chemical composition.

The effects of surface roughness and composition of the substrate on the differentiation of osteoblasts have been studied extensively, as were the factors of cell attachment [43–45]. Deligianni *et al.* employed three types of HA with different surface roughnesses, and found no significant difference in the expression of ALP activity [43]. Surface roughness may be negligible with respect to HA because compositional factors are dominant for differentiation of osteoblasts.

Porosity characterization is based on the presence of open pores which are related to properties such as the permeability and surface area of the porous structure. High porosity usually means a high surface area/volume ratio, and thus favors cell adhesion to the scaffold, promotes extracellular matrix (ECM) regeneration, and minimizes diffusion constraints during *in vitro* culture. The porosity of ceramic materials may facilitate the formation of cell clusters [46]. Cell aggregation is an early and critical event leading to cell differentiation and the mineralization process.

In this study, scaffold C had a higher porosity than scaffolds A and B, which may provide a more favorable biological environment. Cells grown on scaffold C showed an elevated ALP activity and a greater rate of proliferation, in comparison with cultures grown on scaffolds A and B. It is likely that this porosity difference contributed to the better osteoblast response noted in scaffold C. The lower porosity of scaffolds A and B may constrain the flow of materials in and out of the matrix bulk. However, the porosity difference noted among all the samples would not alone be expected to produce the observed difference in the biological behavior of these biomaterials.

We could not explain the cell behavior on the materials based on this experiment alone, because there are other factors that influence it, such as the topography and surface energy. Further investigation should be performed in order to gain a better understanding of the mechanism of the observed *in vitro* behavior.

5. Conclusions

Three porous scaffolds were prepared: scaffold C by the three-dimensional gel-lamination method, and scaffolds A and B by sintering of bovine bone. XRD and FT-IR studies confirmed the samples to be hydroxyapatite. SEM examination and mercury porosimetry measurement showed that the pores were interconnected and the pore sizes ranged from several microns to hundreds of microns.

Moreover, the results obtained clearly demonstrated that three types of HA scaffolds showed good attachment, proliferation and differentiation of osteoblasts. The cell proliferation rate and ALP activity were higher on scaffold C, but were similar on scaffolds A and B. Further studies are in progress in order to further investigate these results and to yield a complete interpretation of these events.

In conclusion, the three-dimensional gel-lamination method was proven to be an attractive process to design and fabricate bone scaffolds with favorable properties. The method may easily be used in other ceramic phases and materials, and therefore, has promising potential for bone repair applications. Besides scaffold C prepared using three-dimensional gel-lamination, the biocompatibility of scaffolds A and B prepared by sintering bovine bone also shows their promise as scaffolds for bone tissue engineering.

Acknowledgements Thanks are due to the National Basic Research Program of China (No. 2005 CB623905), Tsinghua-Yue-Yuen Medical Sciences Fund and National Natural Science Foundation of China (No. 30400099), for financial support.

References

1. J. A. KOEMPEL and B. S. PATT, *J. Biomed. Mater. Res.* **41** (1998) 359.
2. M. JARCHO, *Clin. Orthop. Rel. Res.* **157** (1981) 259.
3. H. YAMASAKI, *Jpn. J. Oral. Biol.* **32** (1990) 190.
4. U. RIPAMONTI, *J. Bone. Joint. Surg. Am.* **73** (1991) 692.
5. X. D. ZHANG, In "Bioceramics and the human body" (Amsterdam, Elsevier, 1991) p. 408.
6. H. YUAN and Y. LI, *Biomed. Eng. Appl. Basis. Com.* **9** (1997) 274.
7. M. OKUMURA and H. OHGUSHI, *J. Biomed. Mater. Res.* **37** (1997) 122.
8. C. ZHANG and J. X. WANG, *J. Biomed. Mater. Res.* **55** (2001) 28.
9. M. E. NORMAN and H. M. ELGENDY, *Clin. Mater.* **17** (1994) 85.
10. P. SEPULVEDA, *Am. Ceram. Soc. Bull.* **76** (1997) 61.
11. J. SAGGIO-WOYANSKY and C. E. SCOTT, *Am. Ceram. Soc. Bull.* **71** (1992) 1674.
12. S. JOSCHEK and B. NIES, *Biomaterials*. **21** (2000) 1645.
13. M. SIVAKUMAR and T. S. SAMPATH KUMAR, *Biomaterials.* **17** (1996) 1709.
14. S. GUIZZARDI and M. RASPANTI, *Biomaterials.* **16** (1995) 931.
15. X. Y. WANG and J. M. TIAN, *Key. Engineering. Materials.* **224-2** (2002) 437.
16. H. SUDO and H. A. KODAMA, *J. Cell. Biol.* **96** (1983) 191.
17. J. Y. CHOI and B. H. LEE, *J. Cell. Biochem.* **61** (1996) 609.
18. A. G. MIKOS and M. D. LYMAN, *Biomaterials.* **15** (1994) 55.
19. Y. DENG and K. ZHAO, *Biomaterials.* **23** (2002) 4049.
20. F. CHEN and Z. C. WANG, *Mater. Lett.* **57** (2002) 858.
21. R. N. PANDA and M. F. HSIEH, *J. Phys. Chem. Solids.* **64** (2003) 193.
22. L. M. RODRíGUEZ-LORENZO and J. M. F. FERREIRA, *Mater. Res. Bull.* **39** (2004) 83.
23. J. F. OSBORN, In "Implantatwerkstoff Hydroxylapatitkeramik" (Berlin, Quintessenz Verlags-GmbH, 1985) p. 17–8; 32–6; 39.
24. H. YAMASAKI and H. SAKAI, *Biomaterials*. **13** (1992) 308.
25. P. L. TRANQUILLI and A. MEROLLI, *J. Mater. Sci. Mater. Med.* **5** (1994) 345.
26. L. CHOU and B. MAREK, *Biomaterials*. **20** (1999) 977.
27. P. S. EGGLI and W. MULLER, *Clin. Orthop. Rel. Res.* **232** (1988) 127.
28. R. E. HOLMES and V. MOONEY, *Clin. Orthop. Rel. Res.* **188** (1984) 252.
29. W. J. DHERT and C. P. KLEIN, *J. Biomed. Mater. Res.* **25** (1991) 1183.
30. A. TACHIBANA and Y. FURUTA, *J. Biotechnol.* **93** (2002) 165.
31. E. WINTERMANTEL and J. MAYER, *Biomaterials.* **17** (1996) 83.
32. E. TSURUGA and H. TAKITA, *J. Biochem (Tokyo).* **121** (1997) 317.
33. L. L. HENCH, *J. Am. Ceram. Soc.* **74** (1991) 1487.
34. F. B. BAGAMBISA and U. JOOS, *J. Biomed. Mater. Res.* **27** (1993) 1047.
35. C. P. KLEIN and A. A. DRIESSEN, *J. Biomed. Mater. Res.* **17** (1983) 769.
36. P. SEPULVEDA and F. S. ORTEGA, *J. Am. Ceram. Soc.* **83** (2000) 3021.
37. L. J. GIBSON and M. F. ASHBY, In "Cellular solids: structure and properties. Cambridge solid state science series, 2 nd Ed" (Cambridge, UK, Cambridge University Press, 1997) p. 429.
38. W. C. VROUWENVELDER and C. G. GROOT, *Biomaterials.* **13** (1992) 382.
39. P. J. MARIE, *Calcif. Tissue. Int.* **56** Suppl 1 (1995) S13.
40. D. A. PULEO and L. A. HOLLERAN, *J. Biomed. Mater. Res.* **25** (1991) 711.
41. M. HOTT and B. NOEL, *J. Biomed. Mater. Res.* **37** (1997) 508.
42. H. ZREIQAT and P. EVANS, *J. Biomed. Mater. Res.* **44** (1999) 389.
43. D. D. DELIGIANNI and N. D. KATSALA, *Biomaterials.* **22** (2001) 87.
44. K. HATANO and H. INOUE, *Bone.* **25** (1999) 439.
45. J. Y. MARTIN and Z. SCHWARTZ, *J. Biomed. Mater. Res.* **29** (1995) 389.
46. J. C. DUBOIS and C. SOUCHIER, *Biomaterials.* **20** (1999) 1841.